

## EVALUATION OF ZY1-02D HYPERSPECTRAL SATELLITE SURFACE REFLECTANCE PRODUCTS

Shuhan Liu<sup>1</sup>, Li Guo<sup>1,\*</sup>, Bai Xue<sup>1</sup>, Xia Wang<sup>1</sup>, Hao Zhang<sup>2</sup>, Hongwei Zhang<sup>3</sup>

<sup>1</sup> Land Satellite Remote Sensing Application Center, MNR

<sup>2</sup> Aerospace Information Research Institute, Chinese Academy of Sciences

<sup>3</sup> China University of Mining and Technology

\*Corresponding author, e-mail address: coaqtig@163.com

Commission III, WG III/4

**KEY WORDS:** ZY1-02D satellite, Hyperspectral, Surface reflectance, Accuracy evaluation

### ABSTRACT:

ZY-1 02D satellite is an important satellite in China space infrastructure planning. The Land Satellite Remote Sensing Application Center of the Ministry of Natural Resources of the People's Republic of China (LASAC) undertook the construction of the satellite hyperspectral data processing system and produced surface reflectance products. Reflectance is the basis of hyperspectral remote sensing data application, which is directly related to the efficiency and quality of hyperspectral application. At present, there is no comprehensive and in-depth study on the accuracy evaluation of the atmospheric correction reflectance of ZY1 - 02D satellite hyperspectral data. In view of this problem, Accuracy Verification of LASAC products using accuracy, precision, uncertainty, spectral curve correlation and spectral angle chord four indicators based on surface reflectance produced by AERONET ground measured data. The results show that the average values of accuracy, precision, uncertainty of LASAC products are 3.2 %, 2.02 % and 4.13 %, respectively. The spectral curve correlation and spectral chord angle are 0.998 and 0.979, respectively. The research result can provide technical reference for the processing and application of ZY1 - 02D hyperspectral image surface reflectance products.

### 1. INTRODUCTION

Hyperspectral remote sensing technology is a new type of earth observation technology in the 1980s (Claverie et al., 2015). It began with the development of imaging spectrometer technology (Santamaria-Artigas et al., 2021). Like microwave, laser and high spatial resolution remote sensing, hyperspectral remote sensing is a hot topic in the field of remote sensing since the new century (Xie et al., 2022). Compared with traditional remote sensing, hyperspectral remote sensing is a continuous remote sensing imaging technique using very narrow and continuous spectral channels on the ground (Yi et al., 2008). Its resolution can reach nanometer order of magnitude. The number of spectral channels is up to tens to hundreds, and the spectral channels are often continuous (Yi et al., 2008). Compared with multispectral remote sensing, hyperspectral remote sensing has higher spectral resolution and can easily obtain more spectral information, which makes the geometric characteristics and texture information of ground targets more prominent (Litvinov et al., 2012). It provides a basis for remote sensing technology from qualitative analysis to quantitative analysis (Sun et al., 2017). Although the spectral resolution of the obtained remote sensing data is getting higher and higher, in the process of image data acquisition, it is inevitably affected by atmospheric, light and other factors, so the obtained data still cannot accurately express the ground object information. Therefore, before the hyperspectral remote sensing data are put into application, the image must be corrected first, mainly including radiometric calibration and atmospheric correction, so as to reduce or eliminate the influence of atmosphere and cloud on the image and reduce the error. In this experiment, the surface

reflectance product generated based on AERONET (Wang et al., 2011) site is used as the true value to verify the surface reflectance product produced by LASAC. The verification methods include band-by-band verification and spectral similarity verification. It lays the foundation for the subsequent application of ZY1 - 02D satellite hyperspectral image fusion and classification.

### 2. DATA

#### 2.1 ZY1-02D

ZY1-02D satellite was successfully launched on September 12, 2019 and was constructed under the chairmanship of the Ministry of Natural Resources. It belongs to the medium resolution remote sensing operational satellite of space-based planning. The satellite has an AHSI hyperspectral sensor with a hyperspectral resolution of 30 meters, 166 bands and a width of 60 km. It has 76 bands in visible and near infrared light, and the spectral resolution is 10 nm; in short-wave infrared there are 90 bands, spectral resolution of 20 nm. In addition, the satellite also has a panchromatic of 2.5m and a multispectral of 10m, with a width of 115km, and the multispectral has 8 bands. On the basis of undertaking the capability of 02C satellite, ZY1-02D satellite has comprehensively improved the functional performance of the satellite in terms of attitude and image quality. Among them, the multispectral spectrum is expanded from 4 to 8, and the width is doubled; Hyperspectral camera fully inherits the mature technology of "GF5" hyperspectral camera, and further optimizes it according to the business needs of the main body of natural resources. Some core indicators

\* Corresponding author.

E-mail address: coaqtig@163.com (Li Guo)

such as signal-to-noise ratio are at the international leading level. The parameters of ZY1-02D are shown in Table 1.

Project		Parameter		
Visible / Near infrared camera	Spectral Range	B01	0.452-0.902 $\mu\text{m}$	
		B02	0.452-0.521 $\mu\text{m}$	
		B03	0.522-0.607 $\mu\text{m}$	
		B04	0.635-0.694 $\mu\text{m}$	
		B05	0.776-0.895 $\mu\text{m}$	
		B06	0.416-0.452 $\mu\text{m}$	
		B07	0.591-0.633 $\mu\text{m}$	
		B08	0.708-0.752 $\mu\text{m}$	
		B09	0.871-1.047 $\mu\text{m}$	
Spatial Resolution	B01	2.5m		
	B02- B09	10m		
Width	115km			
Hyperspectr al camera	Spectral Range	0.40-2.50 $\mu\text{m}$ ; 166 bands in total		
	Spatial Resolution	30m		
	Spectral Resolution	Visible near infrared	10nm	
		Shortwave infrared	20nm	
Width	60km			
Side Swing Ability	26			
Revisit Time	3 days			
Global Coverage Ability	55 days			

**Table 1.** Parameters of ZY1-02D

The successful launch and operation of ZY1-02D satellite will further expand the technical means of natural resources investigation and monitoring in China, greatly improve the ability of quantitative investigation and monitoring of natural resources such as mountains, rivers, forests, fields, lakes and grasses, support and timely control the quantity, quality, ecological status and change trend of natural resources. ZY1-02D satellite can play an important role in ecological environment monitoring and soil quality assessment. It is an important scientific and technological support to promote the high-quality development of natural resources, and can be widely used in emergency management, ecological environment and other related fields by the higher spectral resolution of the satellite.

After the ZY1-02D satellite is put into use, it will carry out collaborative observation with GF5 satellite, and form a satellite constellation in land resources with subsequent satellites to further improve the coverage and revisit ability. With the gradual implementation of the national air-based planning and land and sea planning, it is estimated that by 2025, in the field of natural resources, we will gradually build land middle constellation and high score constellation, covering panchromatic, multispectral, hyperspectral, SAR, lidar and other loads, form an all-weather and full spectrum remote sensing data support system. It lays a foundation for the construction of natural resources investigation and supervision system of heaven and earth integration in China.

## 2.2 AERONET

AERONET is a ground-based aerosol monitoring network established by NASA to monitor global aerosol characteristics. The monitoring network has developed so far and has multiple sites worldwide. Since AERONET adopts the same observation instrument and aerosol inversion algorithm, its inversion accuracy is basically the same worldwide. In addition, due to the data products after strict processing and review that had high precision, usually used as a true value. Considering that the time point distribution of level-1.5 AERONET data is more uniform and dense, level-1.5 aerosol optical thickness product is used to verify the accuracy of aerosol optical thickness. In the experiment, the ground AERONET observation data which is close to the transit time of ZY1-02D data is selected. Figure 1 for details.



**Figure 1.** AERONET data website

## 3. METHOD

The accuracy of reflectance products can be tested by direct, indirect or comparative verification (Wang et al., 2021). The direct accuracy test method is to measure the reflectance of the uniform surface area at the same time in the satellite transit (Revuelto et al., 2021), and calculate the similarity or root mean square error between the reflectance of the image inversion and the measured reflectance to reflect the accuracy of the inversion results. Indirect validation is to obtain surface reflectance by comparing other quasi-synchronous satellite reflectance products or atmospheric correction using measured atmospheric data at ground stations (Vermote et al., 2014). The verification methods include band-by-band verification and spectral similarity verification. Three statistics (accuracy, precision and uncertainty) can be used to describe the band-by-band verification. The calculation formula is as follows:

$$\begin{aligned}
 A &= \frac{1}{n} \sum_{i=1}^n (\rho_i^e - \rho_i^t) \\
 P^2 &= \frac{1}{n-1} \sum_{i=1}^n (\rho_i^e - \rho_i^t - A)^2 \\
 U^2 &= \frac{1}{n} \sum_{i=1}^n (\rho_i^e - \rho_i^t)^2
 \end{aligned} \tag{1}$$

n is the number of samples used for comparison (i.e. the number of pixels);  $\rho_i^e$  is the reflectance to be verified;  $\rho_i^t$  is the true reflectance; Among the three statistics, the first statistic A is used as the quantization average error; The second statistic P is used to characterize the dispersion degree of the error; U represents root mean square error. The higher the value of A, P and U, the worse the consistency between the verification set and the set to be verified, while the lower the value, the better the matching relationship between the two data sets.

During verification, the pixels in different bands are divided into the following intervals according to the reflectance for verification: 0 % – 5 %, 5 % – 10 %, 10 % – 15 %, 15 % – 20 %, 20 % – 25 %, 25 % – 30 %, 30 % – 35 %, 35 % – 40 %, > 40 %. When evaluating the spectral similarity, the spectral cosine angle and correlation coefficient are used to characterize the accuracy.

$$\cos\theta = \frac{\sum_{i=1}^n x_i y_i}{\sqrt{\sum_{i=1}^n x_i^2} \sqrt{\sum_{i=1}^n y_i^2}}, \theta \in [0, \frac{\pi}{2}] \quad (2)$$

$$r = \frac{\sum_{i=1}^n (x_i - \bar{x})(y_i - \bar{y})}{\sqrt{\sum_{i=1}^n (x_i - \bar{x})^2} \sqrt{\sum_{i=1}^n (y_i - \bar{y})^2}} \quad (3)$$

$X_i$  and  $Y_i$  are reflectance values corresponding to different wavelengths of spectral curve to be verified and true value spectral curve respectively.  $\bar{X}$  and  $\bar{Y}$  are the average values of these reflectance, respectively. The value range of spectral angle cosine  $\cos\theta$  and correlation coefficient r is [0,1]. The larger the value, the more similar the two spectral curves are and the better the accuracy verification results are.

#### 4. EXPERIMENTS

The experimental flow chart is as follows, including data screening, reflectance production, data processing and accuracy verification. Figure 3 for details.

##### 4.1 Data Screening

Since the use of AERONET data needs to be synchronized with satellite observation time, ZY1-02D data is filtered based on the center latitude and longitude of AERONET site and data acquisition time. Finally, 14 ZY1-02D images in China area were selected. The data are mainly evenly distributed in the southeast of Hu Line and include Tibet to the north. The data acquisition is relatively comprehensive. Figure 2 for details.

##### 4.2 Reflectance production

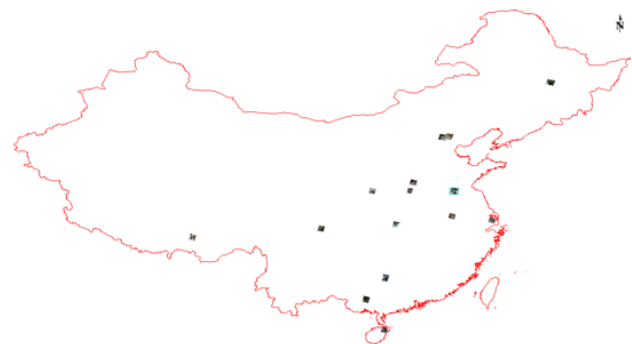


Figure 2. Distribution of ZY1-02D experimental images

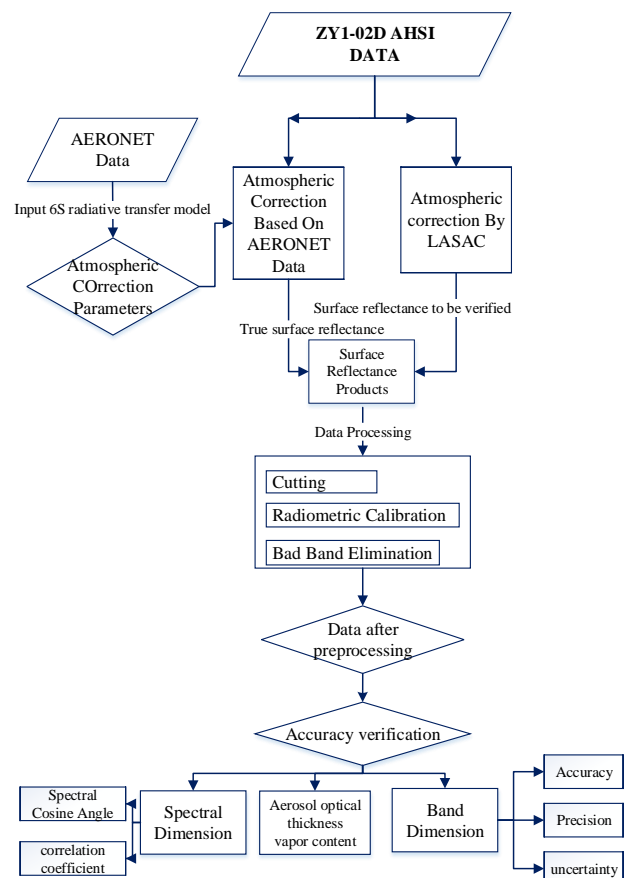


Figure 3. Experimental flow chart

**4.2.1 Production of true reflectance products based on AERONET:** Equations should be numbered consecutively throughout the paper. The equation number is enclosed in parentheses and placed flush right. Leave one blank lines before and after equations: The AOD, vapor data and observation geometry and imaging time data provided in the original image data observed from AERONET data are input into the 6S radiative transfer model as parameters, and the atmospheric correction parameters are obtained by running the 6S model. The final reflectance product is obtained by atmospheric correction of image with obtained atmospheric correction parameters. In the accuracy verification, the reflectivity is taken as the true value.

**4.2.2 Generation of LASAC surface reflectance products:** LASAC surface reflectance calculation process integrates dark pixel extraction, visibility inversion, water vapor inversion and other processes, including the establishment of various look-up tables, and finally completes the surface reflectance calculation of the whole image. Based on dark pixel algorithm extracts water vapor and visibility in the corresponding area of the image data, use atmospheric correction lookup table constructed by prior simulation calculation to calculate the surface reflectance of the area corresponding to the image and generate surface reflectance image

### 4.3 Data Processing

**4.3.1 Cutting:** AERONET data is valid for only 10 km around it. In order to ensure accuracy, this experiment takes the site as the center, and chooses the range of 5km \* 5km to cut the data. Figure 4 for details.

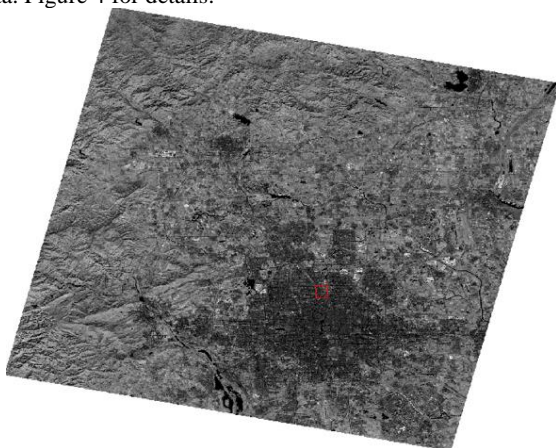


**Figure 4.** Comparison of image size before and after clipping (the image after clipping is in the red box)

**4.3.2 Bad band elimination:** The spectral curve of typical ground objects is viewed on the image, and the strong absorption band of water vapor and the band with frequent negative values are eliminated. The signal-to-noise ratio of these bands is low, and there is no significance for accuracy verification. Finally determined : ZY1-02D data excluding band number : 1-3 ; 98-101 ; 125-133 ; 165-166, a total of 18 bands.

**4.3.3 Elimination of some features:** The reflectance of water, snow and cloud on the image is often not stable or abnormal. Before the accuracy verification, these parts need to be masked.

### 4.4 Accuracy verification

Verify the accuracy of the data after eliminating bad bands. After band elimination, ZY1-02D data have 148 bands and there are about 50,000 effective pixels in each band. Figure 5 for details.

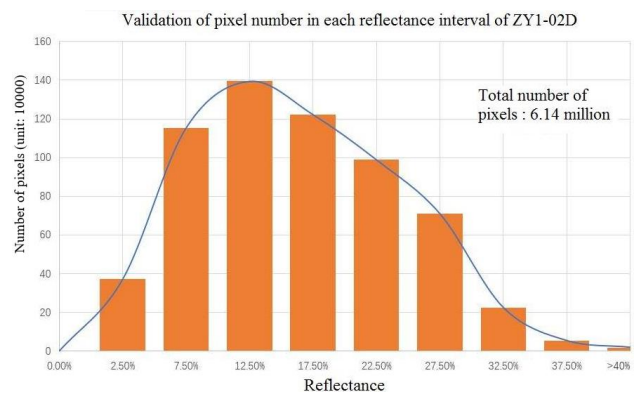


**Figure 5.** Validation of pixel number in each reflectance interval of ZY1-02D

## 5. RESULTS

The experimental results are divided into two parts : the accuracy verification results of reflectance products and the spectral curve display of reflectance products. ZY1-02D band by band verification results are shown in Table 1; the verification results of spectral dimension are shown in Table 2. In different reflectivity ranges, the highest accuracy of LASAC ZY1E reflectance products is 0.21%, the lowest is 6.55%, and the average value is 3.2%; the highest precision of LASAC ZY1E reflectance products is 0.96%, the lowest is 3.37%, and the average value is 2.16%; the highest uncertainty of LASAC ZY1E reflectance products is 1.19%, the lowest is 7.78%, and the average value is 4.48%; The spectral curve correlation and spectral cosine angle are 0.998 and 0.979, respectively. Table 2 and 3 for details.

	0%-5%	5%-10%	10%-15%	15%-20%	20%-25%	25%-30%	30%-35%	35%-40%	>40%
Accuracy	0.21%	1.33%	2.00%	2.49%	3.03%	3.68%	4.15%	5.38%	6.55%
Precision	0.96%	1.16%	1.20%	1.45%	1.82%	2.12%	2.68%	3.40%	3.37%
Uncertainty	1.19%	1.94%	2.53%	3.12%	3.86%	4.63%	5.33%	6.76%	7.78%
Pixel Number	371614	1154635	1395461	1222748	989037	710454	224962	53998	19174

**Table 2.** Reflectance product index

The spectral curves of typical ground objects are shown in Figure 3-5. It can be seen that the reflectance product of this module has a good correlation with the true value data in the spectral dimension. (The red curve in the figure is the reflectance spectrum curve based on AERONET site, and the blue curve is the reflectance spectrum curve obtained by this module ; ZY1-02D amplification coefficient is 1000 ). Figure 6-8 for details.

Directly calculate the error between aerosol optical thickness and water vapor content and measured value to verify the accuracy of aerosol and water vapor retrieval products. The specific verification results are shown in the table below. Table 4 for details.

	Correlation of spectral curves	Spectral Angle Chord Value
<b>Beijing</b>	0.99877	0.99344
<b>Chengdu</b>	0.99894	0.99441
<b>Shanghai</b>	0.99794	0.89341
<b>Nanning</b>	0.99588	0.99049
<b>Zhangye</b>	0.99862	0.995
<b>Xuzhou</b>	0.99659	0.99323
<b>Songshan</b>	0.99945	0.99697
<b>mean</b>	0.998027	0.979564

**Table 3.** Correlation and spectral cosine angle of continuous spectral curve of ZY1-02D reflectance product

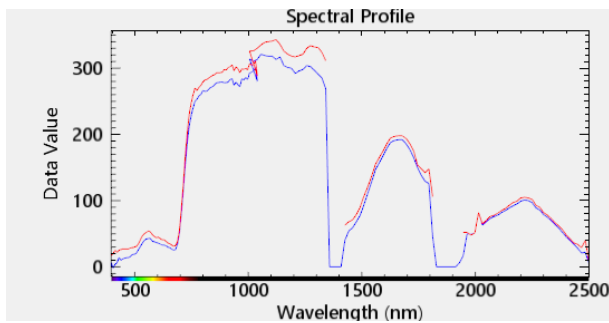


**Figure 6.** Comparison of ZY1-02D vegetation spectral curve

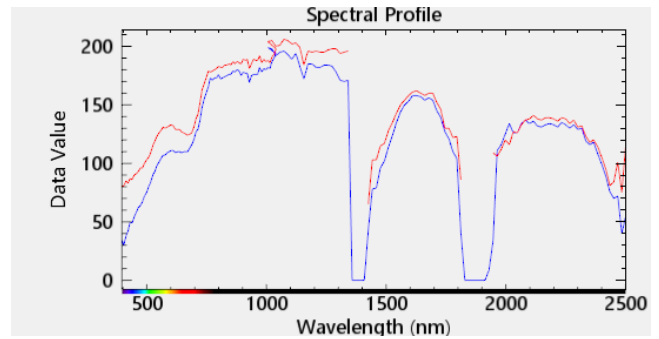


**Figure 7.** Spectral curve comparison of ZY1-02D buildings

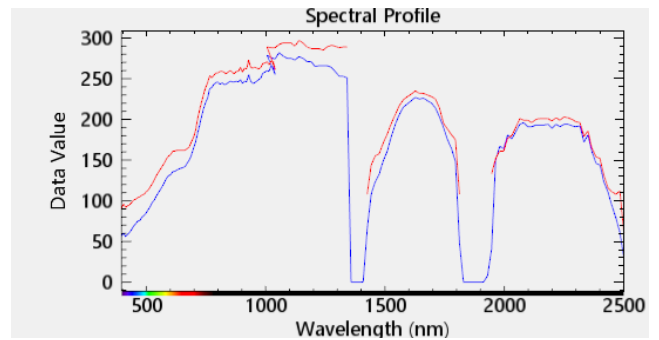


**Figure 8.** Spectral curve comparison of ZY1-02D bare land

	Measured aerosol optical thickness	Aerosol optical depth inversion value	Measured value of water vapor	Water vapor inversion value
Guilin	0.787153	0.685368	4.014822	3.212683
Harbin	0.3937	0.2911	0.9125	1.3405
Hefei	0.224398	0.222198	0.583065	0.631153
Jiaozuo	0.5947	0.3788	0.5041	0.56
Lasa	0.058807	0.065824	0.13846	0.137017
Minqin	0.062147	0.061152	0.299734	0.280697
Zhangye	0.2966	0.3556	0.3065	0.2027
Xian	0.198584	0.190124	0.243146	0.239489
Zhoushan	0.092814	0.098568	5.181224	4.144977
Beijing	0.101156	0.096582	1.493746	1.511164
mean	0.281006	0.244532	1.36773	1.226038

**Table 4.** Accuracy verification of aerosol optical thickness and water vapor inversion

## 6. CONCLUSIONS

Based on the reflectance products generated by AERONET ground measured data, this experiment verifies the accuracy of ZY1-02D reflectance products produced by this module in Beijing, Chengdu and other places, and obtains the following conclusions:

- 1) The accuracy of ZY1 - 02D reflectance products produced by this module in different reflectance ranges is the highest of 0.21 %, the lowest of 6.55 %, and the average of 3.2 %.
- 2) The spectral curve correlation and spectral chord angle of ZY1-02D reflectance product produced by this module are 0.998 and 0.979, respectively.
- 3) The average accuracy and uncertainty of ZY1 - 02D reflectance products produced by this module are 2.02 % and 4.13 %, respectively, showing good performance.

4) The reflectance products produced by this module have highly close to the true values on typical ground objects such as vegetation, buildings and bare land, and the curve is relatively smooth as a whole. Sensing, 63, 661-677, <https://doi.org/10.1016/j.isprsjprs.2008.04.004>, 2008.

## REFERENCES

Claverie, M., Vermote, E. F., Franch, B., and Masek, J. G.: Evaluation of the Landsat-5 TM and Landsat-7 ETM+ surface reflectance products, *Remote Sensing of Environment*, 169, 390-403, <https://doi.org/10.1016/j.rse.2015.08.030>, 2015.

Litvinov, P., Hasekamp, O., Dubovik, O., and Cairns, B.: Model for land surface reflectance treatment: Physical derivation, application for bare soil and evaluation on airborne and satellite measurements, *Journal of Quantitative Spectroscopy and Radiative Transfer*, 113, 2023-2039, <https://doi.org/10.1016/j.jqsrt.2012.06.027>, 2012.

Revuelto, J., Cluzet, B., Duran, N., Fructus, M., Lafaysse, M., Cosme, E., and Dumont, M.: Assimilation of surface reflectance in snow simulations: Impact on bulk snow variables, *Journal of Hydrology*, 603, 126966, <https://doi.org/10.1016/j.jhydrol.2021.126966>, 2021.

Santamaria-Artigas, A., Vermote, E. F., Franch, B., Roger, J.-C., and Skakun, S.: Evaluation of the AVHRR surface reflectance long term data record between 1984 and 2011, *International Journal of Applied Earth Observation and Geoinformation*, 98, 102317, <https://doi.org/10.1016/j.jag.2021.102317>, 2021.

Sun, Q., Wang, Z., Li, Z., Erb, A., and Schaaf, C. B.: Evaluation of the global MODIS 30 arc-second spatially and temporally complete snow-free land surface albedo and reflectance anisotropy dataset, *International Journal of Applied Earth Observation and Geoinformation*, 58, 36-49, <https://doi.org/10.1016/j.jag.2017.01.011>, 2017.

Vermote, E., Justice, C., and Csiszar, I.: Early evaluation of the VIIRS calibration, cloud mask and surface reflectance Earth data records, *Remote Sensing of Environment*, 148, 134-145, <https://doi.org/10.1016/j.rse.2014.03.028>, 2014.

Wang, T., Melton, F. S., Pôças, I., Johnson, L. F., Thao, T., Post, K., and Cassel-Sharma, F.: Evaluation of crop coefficient and evapotranspiration data for sugar beets from landsat surface reflectances using micrometeorological measurements and weighing lysimetry, *Agricultural Water Management*, 244, 106533, <https://doi.org/10.1016/j.agwat.2020.106533>, 2021.

Wang, Y., Czapla-Myers, J., Lyapustin, A., Thome, K., and Dutton, E. G.: AERONET-based surface reflectance validation network (ASRVN) data evaluation: Case study for railroad valley calibration site, *Remote Sensing of Environment*, 115, 2710-2717, <https://doi.org/10.1016/j.rse.2011.06.011>, 2011.

Xie, S., Liu, L., and Yang, J.: Enhanced Landsat surface reflectance prediction considering land cover change by using an ensemble of spectro-temporal and spectro-spatial predictions, *Advances in Space Research*, <https://doi.org/10.1016/j.asr.2022.01.009>, 2022.

Yi, Y., Yang, D., Huang, J., and Chen, D.: Evaluation of MODIS surface reflectance products for wheat leaf area index (LAI) retrieval, *ISPRS Journal of Photogrammetry and Remote*